COMPARISON OF PREDICTION AND PERFORMANCE FOR A 62m SPAN SPORTS HALL IN JOINTED GNEISS

N. BARTON – T.L. BY – P. CHRYSSANTHAKIS – L. TUNBRIDGE – J. KRISTIANSEN – F. LØSET – R.K. BHASIN – H. WESTERDAHL – G. VIK

Norwegian Geotechnical Institute, Oslo, Norway

ABSTRACT

The feasibility of excavating caverns of very large span for underground location of a nuclear power station in Norway was investigated in the early 1970s. In the end, the 1994 Winter Olympic Games has provided the necessary impetus for utilising very large engineered rock caverns. The 62m span Olympic Ice Hockey cavern has been constructed in Gjøvik, Norway. It is located in jointed gneiss of average RQD = 70% and has a rock cover of only 25 to 50m, thus posing challenging design problems. The investigations prior to construction included two types of stress measurements, cross-hole seismic tomography, special core logging, Q-system classification and numerical modelling with UDEC-BB. Predicted maximum deformations were 4 to 8mm; surprisingly small due to the high horizontal stresses recorded. Extensometer (MPBX) installations from the surface prior to construction, precision surface levelling and MPBX installed from inside the cavern give a combined measure of maximum deformations in the range 7 to 8mm with the 62m span fully excavated, and three adjacent caverns for the Postal Services also completed.

INTRODUCTION

During the 1970s, NGI performed a series of siting studies and some *in situ* testing, to investigate the feasibility of underground siting of nuclear power plants. Special attention was focused on the need for a reactor containment cavern with a hemispherical domed arch of at least 50m diameter. The Norwegian State Power Board (Statkraft) and subsequently also the Swedish State Power Board (Vattenfall) funded parallel theoretical studies of large span caverns.

The Norwegian Geotechnical Institute (NGI) first performed physical models of large spans in jointed rock, studying the effect of medium and high horizontal stress levels and the effects of various jointing patterns. Comparisons were also made with continuum FEM studies. Today, fifteen years later, we would have used discrete element methods such as UDEC. A brief review of some of the findings of these earlier studies will be used as an introduction to the real life problems subsequently encountered at Gjøvik, where a 62m span cavern has been successfully engineered for the 1994 Winter Olympic Games which will be centred at Lillehammer.

Prior to specific siting of large caverns, whether for nuclear reactor vessels or for Olympic Ice Hockey, estimates have to be made of stress levels and rock properties. Concerning stress levels, we elected to investigate low, medium and high stress as follows:

$$\sigma_h/\sigma_v = 1/3$$
$$\sigma_h/\sigma_v = 1.0$$
$$100/z + 0.3 \le \sigma_h/\sigma_v \le 1500/z + 0.5$$

The latter (where z is depth in metres) is based on measured data reviewed by BROWN & HOEK (1978). The actual level chosen in the third case was k = 20 at 25m depth and k = 6 at 100m depth, i.e., a trapezoidal distribution of stress, within the above range of observations.

Figure 1 illustrates the FEM results obtained with an assumed rock cover of only 25m, E = 14 GPa, υ = 0.1 and ***plane stress*** conditions (equivalent to the two-dimensional physical models). For stage 2 of the excavation (roughly equivalent to the Olympic Ice Hockey cavern dimensions) maximum vertical deformations for the three stress cases were 2.7mm, 1.5mm and (-) 10.8mm (i.e., heave). When the rock cover was increased to 50m, the isotropic case (k = 1.0) showed a maximum downward deformation of 2.9mm, i.e., the tendency for heave is of course reduced.

The physical models, which are described in detail by BARTON & HANSTEEN (1979) consisted of 20,000 blocks of discretely fractured model material, with two regular joint patterns of constant dip. These two-dimensional models were loaded by gravity and by vertical boundaries that resemble today's numerical roller boundaries. Figure 2 illustrates two of the physical model results under stress levels equivalent to those described above. It should be noted that the tension fracturing technique gives the two sets of joints (one continuous, the other discontinuous) unusually high values of JRC (joint roughness coefficient). Stability is therefore ensured in the arch of the models, but not in the walls.

The above numerical and physical models demonstrated the possible favourable nature of near-surface siting for large caverns at least from the point of view of possible high horizontal stress levels and reduced deformation. A compromise would need to be

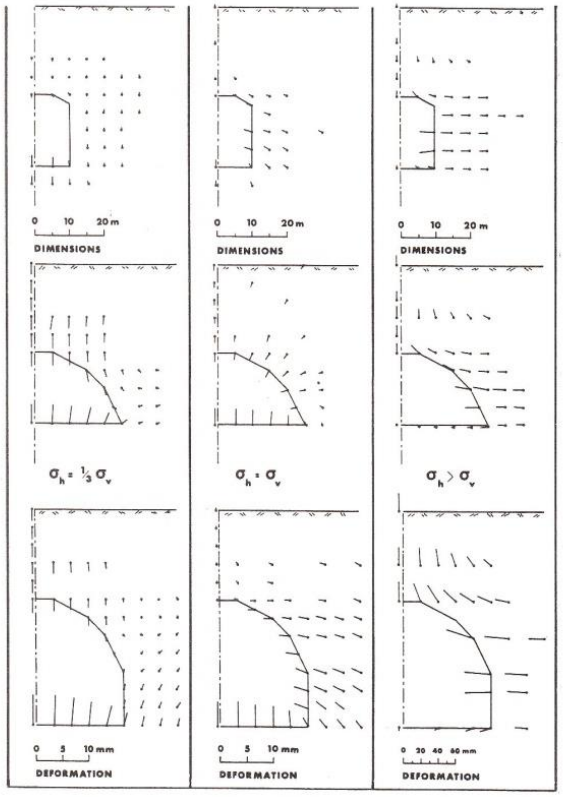

Fig. 1 Displacement vectors obtained from FEM continuum studies of large caverns (BARTON & HANSTEEN, 1979)

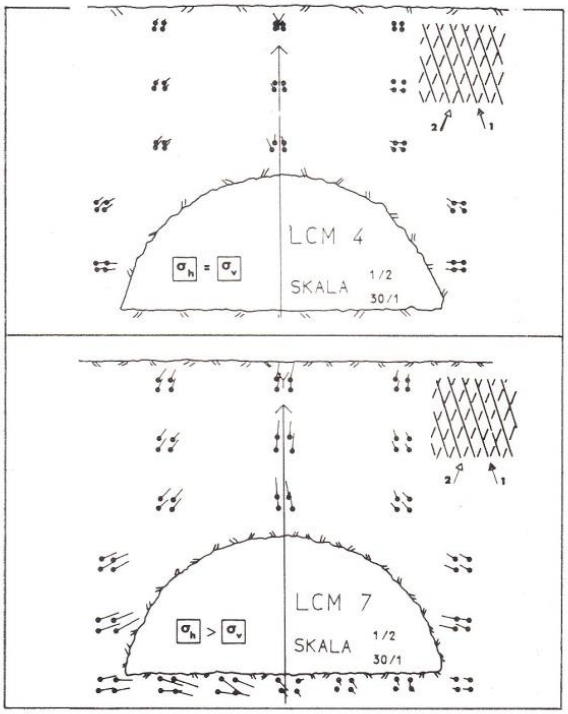

Fig. 2 Displacement vectors obtained from two physical models with jointing as shown (BARTON & HANSTEEN, 1979)

arrived at, involving near-surface siting but avoidance where possible of near-surface weathering and higher joint frequencies.

AN OLYMPIC SPORTS HALL

The idea of locating an Olympic arena in rock was first conceived by Fortifikasjon A/S, who, together with the City of Gjøvik, were responsible for the project development and marketing during the 18 months from when the project was first presented until a contract agreement was reached. As is typical when one is extending the limits of experience and technology, the initial scepticism that had to be overcome was formidable.

The ice hockey cavern was to have a span of 60m, a length of 91m and a height of 24m. The spectator capacity is currently 5,300, making it by far the largest cavern for public use in the world.

In 1991, NGI and NOTEBY of Oslo, and SINTEF/NTH of Trondheim cooperated in a series of geological and rock mechanics investigations with rock cavern designers Fortifikasjon A/S of Oslo as client.

During the first phase of feasibility studies, existing, nearby rock caverns and access tunnels were mapped in the same hillside in the PreCambrian gneiss. Good rock exposures were available in the arch of a nearby swimming pool cavern, in the arch of a parallel cavern housing the changing rooms, and in the nearby Telephone Exchange caverns. This mapping was done in Phase I before drill holes from the surface were available. Figure 3 shows the location of the swimming pool cavern in relation to the ice hockey cavern.

The PreCambrian gneiss had a frequency of jointing perhaps more than in Norwegian basement rocks in general. However, the joints were generally irregular, rough walled, and with quite large variations in dip and strike. The spacing of the more persistent jointing was often several metres. The general joint character was one of low persistence, moderate to marked roughness and without clay filling, i.e., potentially positive characteristics for large spans. The tectonised red gneiss at the site had many short irregular joints. Foliation was poorly developed, but generally had a strike of approximately E-W with a dip of 35° to 55°.

The hillside 25 to 50m above the planned roof of the cavern had a generally smooth relief without marked depressions or traces of weakness zones. However, there was a marked NE-SW, subvertical fault zone crossing the access tunnel portals 50 to 100m from the rock caverns, and affecting the jointing locally.

The most typical rock quality visible in the existing caverns, which are located between 25 and 100m from the proposed site was the following:

$$Q = \frac{90}{6} \times \frac{2}{1} \times \frac{1}{1} = 30$$

(RQD) = 90%, two to three joint sets, smooth undulating joints, no alteration, little water in flow, no stress problems.) The poorer quality rock could not be observed due to areas of shotcrete.

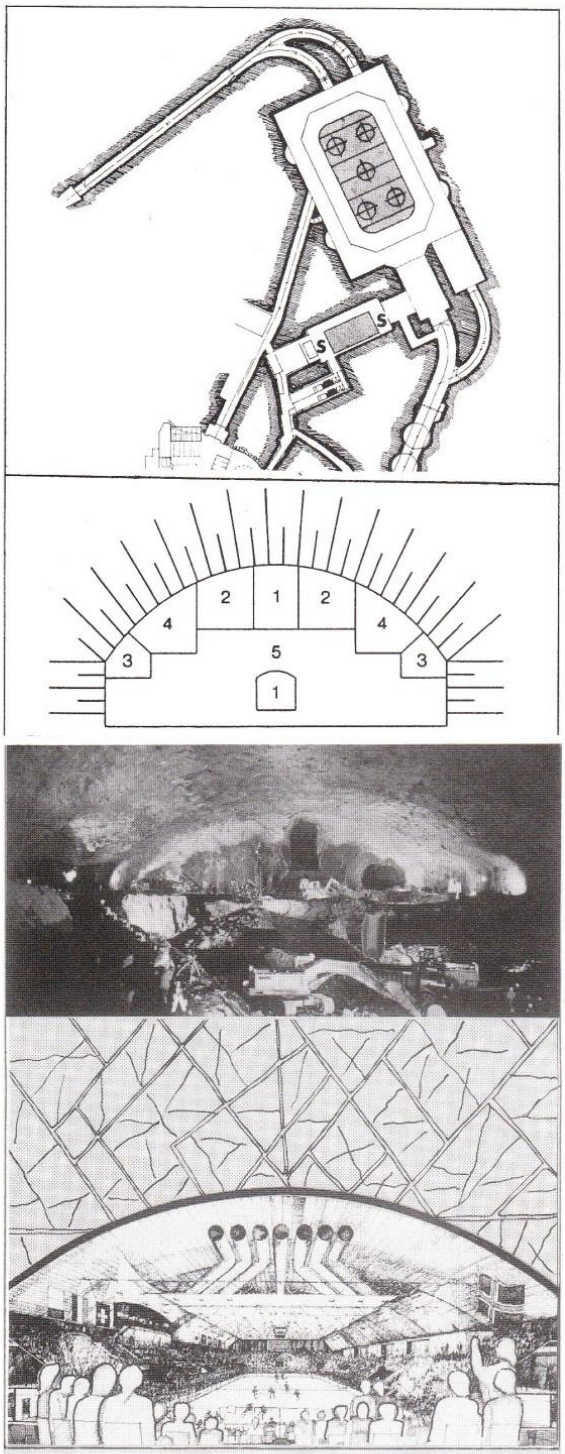

Fig. 3 Cavern layout, existing swimming pool (S), excavation stages, bolting pattern, construction.

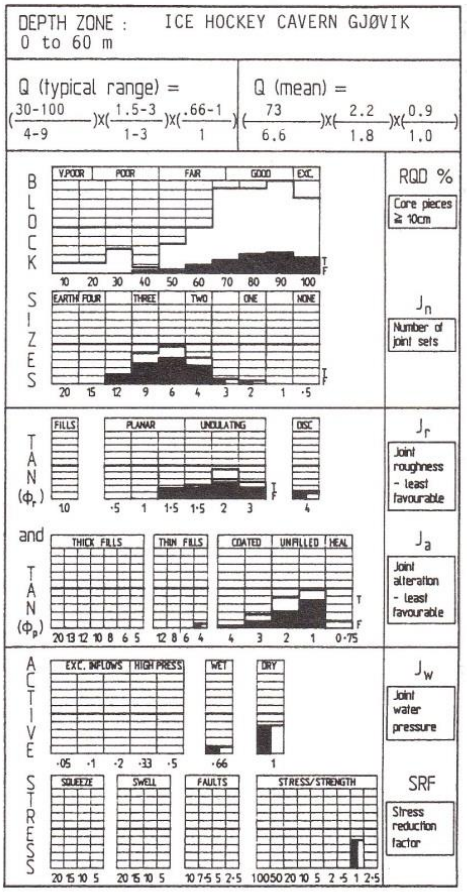

Fig. 4 Independent Q-system characterisation in existing caverns (black). Combined data base with four drill cores included (white).

Figure 4 (black histograms) shows the results of Q-mapping in the existing caverns during Phase I studies.

DRILL CORE ANALYSIS

In Phase II of the investigations, four diamond cored holes of 50 to 70m length were drilled by NOTEBY. Two were vertical and two inclined at 45°, all of them more or less within the potential 90×60m footprint of the cavern, which in practice was nearer 100×100m since cavern orientation had yet to be finalised.

Analysis of joints in the core indicated that a total of five different joint sets could be identified, but these seldom occurred in the same location, and jointing could also be described as sporadic. The most typical dip angles were 50° to 65°, and some 40 to 45% of the joints showed this value. Some 25% of the breaks in the drill core were parallel to foliation, along diffuse planes of weakness. There appeared to be few through-going foliation joints, and their spacing was several metres. Some joints were healed due to mineralization. The most typical joint coatings

or fillings were rust stains, epidote and quartz. Chlorite and calcite coatings occurred occasionally, while clay fillings appeared to be absent.

While part of the core showed evidence of minor brecciated or crushed zones of up to 0.5m in thickness, no core loss or marked alteration were registered. In general the joint frequency (F) was 4 to 8 per metre, but perhaps half the breaks in the core were due to diffuse weakness planes and not technically speaking joints. Through-going, well developed joints generally showed a frequency (F) of only 1 to 3 per metre. RQD was generally in the range 70 to 85%, though 15% of the core had RQD = 100%. A large number of the joints had rough undulating surfaces, especially the foliation joints and the near vertical N-S set of tension joints which probably parallelled the major principal stress.

ROCK MASS CLASSIFICATION

As part of the quality control procedures the first application of the Q-system in the existing rock caverns, and the second application using drill core were carried out by different engineering geologists. As indicated in Figure 4, the two independent assessments were similar. Important minor differences were the observations of some poorer quality rock and coated joints in the drill core logging. Such areas were presumably coated with shotcrete which hindered observation in the cavern mapping.

Based on the combined cavern mapping and core logging the following typical rock qualities are expected in the Olympic Ice Hockey cavern.

1. *Typical best quality* $Q = \frac{90}{6} \times \frac{2}{1} \times \frac{1}{1} = 30$

2. *Typical poorest quality* $Q = \frac{30}{9} \times \frac{1.5}{3} \times \frac{0.66}{1} = 1.1$

The weighted average, obtained from analysis of the complete set of histograms in Figure 4, indicated the following:

3. *Weighted average* $Q = \frac{73}{6.6} \times \frac{2.2}{1.8} \times \frac{0.9}{1.0} = 12$

Figure 5 shows the planned 60m span Ice Hockey cavern plotted on the Q-system rock support diagram. The exceptionally large span and the high safety requirement (ESR = 1.0 to 0.8) places the cavern right at the top or even above the present data base. The need for careful numerical analysis to support the empirically derived reinforcement prediction is evident. Distinct element UDEC-BB analyses (CUNDALL, 1980 and MAKURAT et al. 1990) are described later.

PREDICTION FROM CROSS-HOLE SEISMIC TOMOGRAPHY

Important information for subsequent modelling was obtained from NGI's exploratory cross-hole seismic measurements between vertical boreholes 1 and 3 (approximately 52 metres apart) along the planned long axis of the cavern, and between borehole 3 and the 45° inclined borehole No. 2, along a section perpendicular to the planned axis (BY, 1987). The results of the tomographic analysis for these two profiles are shown in Figure 6.

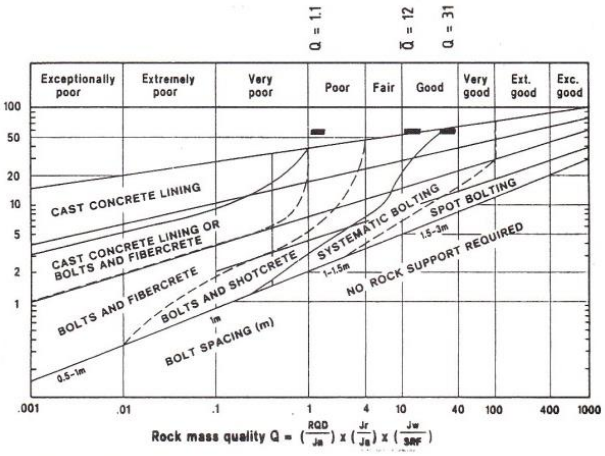

Fig. 5 The 60m span places the Olympic Ice Hockey Cavern at the top of the reinforcement data base (GRIMSTAD et al., 1986)

The P-wave velocity of the rock mass surrounding the cavern, which is located between 151 and 176 m.a.s.l., was generally in the range 5000-5500m/s. In the first 20m above the arch the velocity was somewhat reduced, lying generally in the range 5100m/s down to 3700m/s, with the poorer quality some 10 to 20m above the arch.

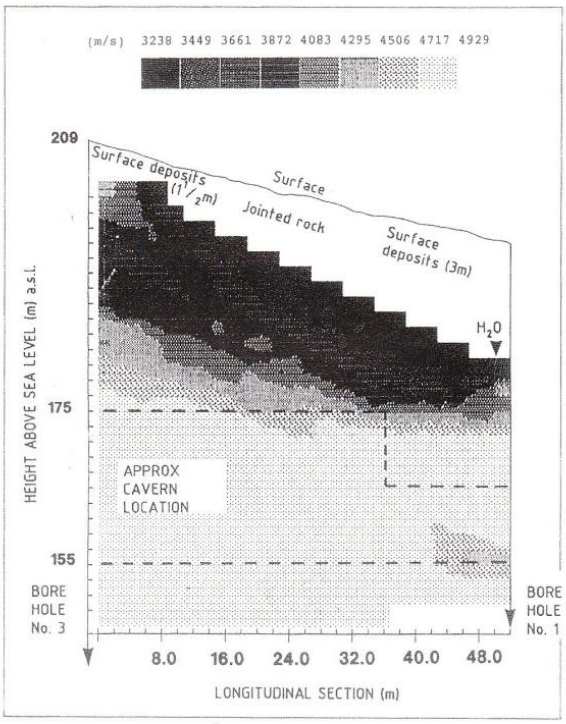

Fig. 6a Cross-hole seismic tomography for longitudinal cross-sections through the cavern site.

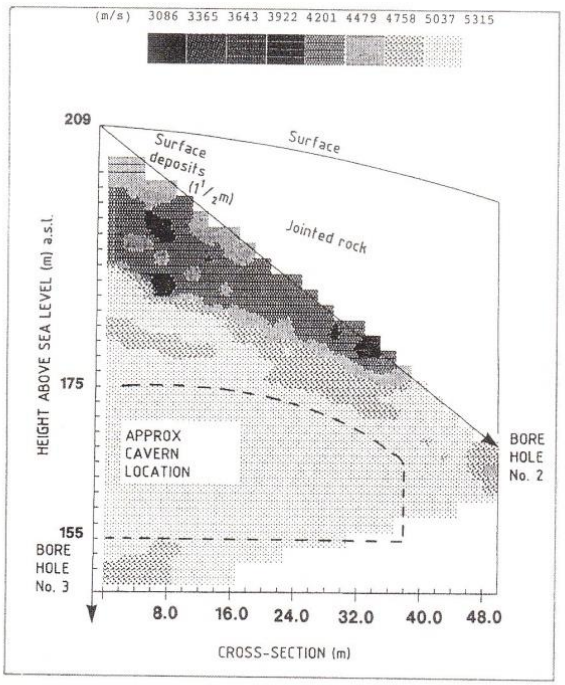

Fig. 6b *Cross-hole seismic tomography for perpendicular cross-sections through the cavern site.*

Detailed comparison between seismic velocity and the local RQD and joint frequency (measured along the drill core) demonstrated good correlation in the shortest vertical hole (No. 1, 45m long). Velocity around 4000m/s at 15m depth corresponded to RQD = 60% and approximately 10 joints per metre. At 40m depth, velocities of about 5000m/s corresponded to RQD = 90% and 2 joints per metre. The latter corresponded to expected mid-cavern wall conditions (at 156 m.a.s.l.).

A feature of the results that has indicated good correlation between the prognosis and the excavated conditions is the reduced velocity and rock quality predicted at the ends of the caverns. Subsequent Q-system mapping within the cavern indicated mean Q-values reducing from between 13 and 20 in the central areas to about 5 at the East end and between 2 and 5 at the West end.

Detailed comparisons of the recently mapped Q-values in the cavern arch and P-wave velocity distributions obtained from the tomography indicate (for these jointed gneisses) the following approximate ranges:

$$Q = 5 \text{ to } 15 \quad V_p = 3900 \text{ to } 4500 \text{ m/sec}$$
$$Q = 20 \text{ to } 30 \quad V_p = 4700 \text{ to } 5200 \text{ m/sec}$$

An approximately linear relationship: $V_p = 50\,Q + 3600$ (m/s) is indicated from these preliminary results over this limited range of rock qualities. Implications for future use are that tunnel or cavern support might be designed to some level of accuracy based on careful calibration of seismic surveys against rock mass classification.

Combination of the above near-surface data with Q-system application at other shallow sites (BARTON et al. 1992) indicates that the following may be a useful first approximation over a wide spectrum of near-surface rock qualities (and stress levels) including fault zone breccia, clay inter-bedded sandstones, siltstones, thin and thickly bedded sandstones, moderately and heavily jointed gneiss:

$$V_p = 1000 \log Q + 3500 (m/s)$$
$$Q = 10^{\frac{V_p - 3500}{1000}} \qquad (1)$$

The simple, easy-to-remember form of these results is shown in Table 1.

Table 1. Approximate Correlation between Q and P-wave velocity

V_p (m/s)	500	1500	2500	3500	4500	5500	6500
Q	0.001	0.01	0.1	1	10	100	1000

Since the mean value of deformation modulus is given by the approximation E = 25 log Q (see BARTON, 1983), combining this expression with Equation 1 suggests that rock mass deformation modulus can be estimated from:

$$E_{(mean)} = \left(\frac{V_p - 3500}{40}\right) \quad (GPa) \qquad (2)$$

for values of P-wave velocity in excess of 3500 m/sec.

ROCK STRESS MEASURMENTS

Preliminary measurements of rock stress using overcoring were performed by SINTEF, utilising a single short hole drilled from an existing cavern. These Phase I measurements indicated a surprisingly high horizontal major principal stress of about 4 MPa with an E-W orientation. However, these first measurements were carried out very close to an existing cavern.

Subsequent hydraulic fracturing and hydraulic jacking measurements carried out in Phase II by NGI confirmed the generally high horizontal stress levels, but suggested a N-S principal stress orientation (N 170° E), which was consistent with the N-S set of vertical tension joints and Permian dykes in the Oslo-Region to the south.

Due to the frequency of jointing in the upper 30m or so of both holes, no measurements were recorded more than 8 metres above the arch. The major horizontal stress was estimated to be 3.5 MPa, 5 metres above the arch of the planned cavern, and oriented N 174° E (approximately N-S). The intermediate stress estimated from joint jacking tests was estimated to be 2.0 MPa, 5 metres above the arch, and oriented N 084° E (approximately E-W). The vertical stress was calculated to be approximately 1.0 MPa at this same location, some 40m beneath the surface.

Shortly before cavern construction commenced in April, 1991, a further set of hydraulic fracturing stress measurements were made in the upper 30m of rock. The combined data sets are shown in Figure 7. The high stress to within about 10m of the surface is a very positive aspect of the site for ensuring the stability of large span excavations.

Note, however, that the stress is not as high as assumed in NGI's earlier studies of nuclear power plant caverns, as described in the introduction. In one of the cases described, a significant stress intercept at the surface was modelled, which caused cavern heave to be predicted.

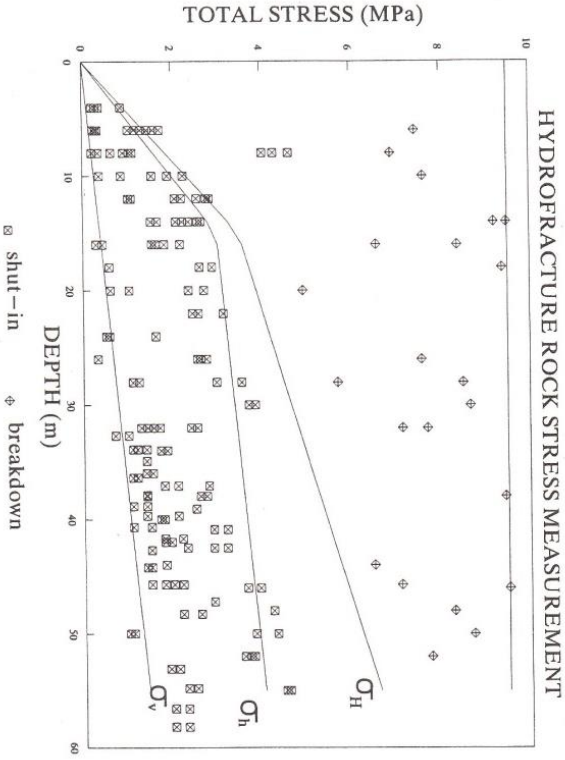

Fig. 7 Results of rock stress measurements using hydraulic fracturing and joint jacking-shut-in.

INPUT PARAMETERS FOR NUMERICAL MODELLING

a) E-Moduli and Uniaxial Strengths

As part of the overcoring stress measurements performed by SINTEF in Phase I studies, the E-modulus and Poisson's ratio of the rock were measured. Mean values were E = 51.5 GPa, υ = 0.21. According to tests on six 61mm diameter samples the unconfined compression strength varied from 63 to 94 MPa reflecting the tectonized nature of the gneiss. In FEM studies performed by NOTEBY, rock mass moduli of 10, 30 and 51.1 GPa were utilised. Maximum predicted arch deformations with 28 and 48m overburden ranged from 20.4mm to 1.6mm with the above range of moduli. Maximum horizontal stresses were mostly in the range 3 to 5 MPa. A similar range of stresses was seen in SINTEF's BEM computations.

b) Deformation Moduli for UDEC Studies

In Phase I studies, NGI utilised both the Q-system and the RMR method of BIENIAWSKI (1976) to estimate the rock mass deformation modulus (BARTON, 1983). The estimated range of values was approximately 10 to 50 GPa, with an average of 30 GPa. This value was used in Phase I UDEC-BB calculations. However, in Phase II, deformation modulus was estimated to take mean values of 20, 30 and 40 GPa, in three increasingly deep zones, as interpreted from drill core and seismic tomography results.

c) Shear Strength Parameters for the Joints

Joint roughness profiles were measured along 1m and 2m long joint surfaces in the existing rock caverns, and gave an approximate indication of large scale waviness, with average (i) values of about 6°. The smaller scale features of joint roughness were measured by performing tilt tests on 101 of the joints recovered in the four drill cores. The most typical value of JRC_0 (joint roughness coefficient, laboratory scale) was about 7.0. When corrected for block-size (approximately 0.5m *in situ*) the large scale value of JRC_n was 5.2.

Following BARTON & BANDIS (1990), the following assumptions were made concerning the peak friction angles for joints with small scale roughness (without undulations) and for joints with large scale roughness (with undulations that could not be sheared through):

1. *Laboratory scale* $\phi_l = JRC_0 \log \dfrac{JCS_0}{\sigma_n} + \phi_r$ (3)

2. *Field scale* $\phi_f = JRC_n \log \dfrac{JCS_n}{\sigma_n} + \phi_r + i$ (4)

where σ_n is the effective normal stress.

Input parameters for the Barton-Bandis (BB) joint behaviour subroutine that is used in NGI's version of Cundall's distinct element two-dimensional (i.e., conservative) code (UDEC-BB) were as follows (MAKURAT et al. 1990):

JRC_0 = 7.5 σ_c = 100 MPa L_n = 0.5 m
JCS_0 = 75 MPa
ϕ_r = 27°
i = 6°

With these input data, a BB-Lotus model was used to produce graphical presentations of coupled shear stress-displacement-dilation-conductivity and normal stress-closure conductivity behaviour. These plots are subsequently used to interpret the graphical output from UDEC-BB; for example the importance or otherwise of 1 or 2mm of joint shearing; has the particular wedge-shaped block reached peak strength; has dilation started; is the conducting aperture reasonable, etc., etc.?

UDEC-BB MODELLING (PHASE I)

A simplified joint geometry was assumed in the first phase of two-dimensional scoping exercises, based solely on joint mapping performed in the existing caverns. Core was not available, and over-coring stress measurements were assumed to be unreliable due to nearness to an existing cavern. For this reason a range of horizontal stress levels was assumed($k_0 = \sigma_h/\sigma_v$ = 0.5, 1.0, 3.0). Two conjugate sets of jointing of limited length were assumed as representative of the observed jointing.

Stresses and displacements following completed (3 stage) excavation of the 60m span simulated cavern are as shown in Figures 8 and 9. Table 2 indicates maximum deformations for the three stages of cavern excavation, with the three levels of assumed horizontal stress discussed above.

The very positive effect of high horizontal stress levels and the equally negative effect of low horizontal stress levels were clear from these preliminary runs, and confirm early physical models and FEM studies reported by BARTON & HANSTEEN (1979). Under certain conditions of cavern dimension, thickness of arch,

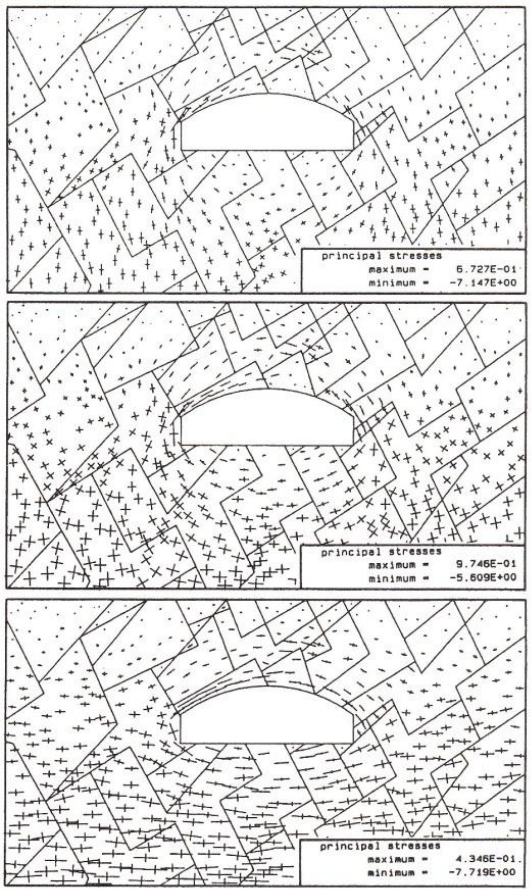

Fig. 8 Simplified Phase I UDEC-BB runs. Principal stresses with k = 0.5, 1 and 3.

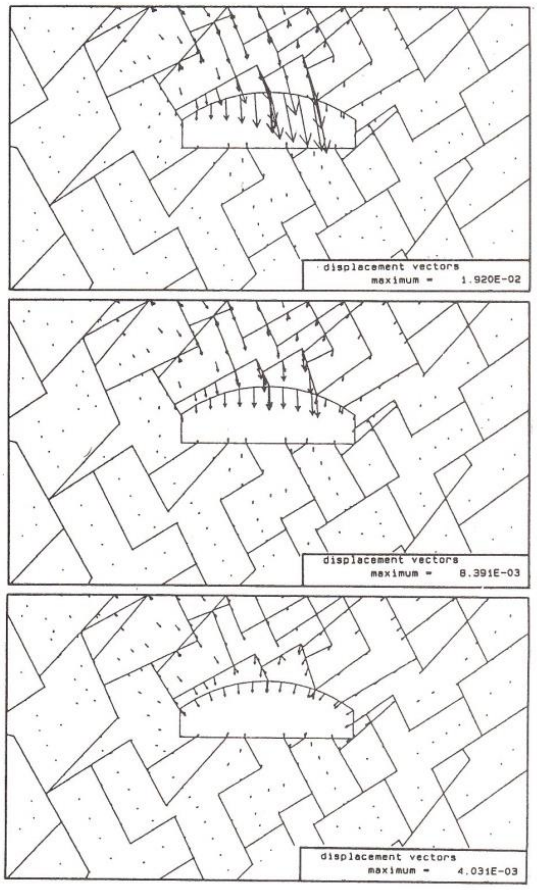

Fig. 9 Simplified Phase I UDEC-BB runs. Deformation vectors, with k = 0.5, 1 and 3 (maximum = 19.2mm)

horizontal stress level and joint orientation, heave of the arch can in fact occur. The ideal for minimizing joint shearing might appear to be a design more or less "in balance" between downwards and upwards oriented deformation. However, slight joint shearing (to mobilize resistance) might be considered even more advantageous. In view of the very large span, the 4mm of deformation recorded with k = 3 must be considered nearly "in balance".

Table 2. Maximum deformations recorded in Phase I UDEC-BB studies, with simplified jointing and only three excavation stages

Cavern dimensions (m)	k = 0.5 (mm)	k = 1.0 (mm)	k = 3 (mm)
20 x 10	0.64	0.61	0.65
60 x 10	19.5	4.2	3.7
60 x 20	19.2	8.4	4.0

The large deformation (19.2mm) recorded in the model with lowest k_o was caused primarily by major joint shearing on the right hand side of the two wedges in the arch. This movement stabilised due to joint dilation and build-up of normal stress, despite lack of modelled bolting in these preliminary studies.

UDEC-BB MODELLING (PHASE II)

The second phase of UDEC modelling was performed following the core drilling, stress measurement and cross-hole seismic tomography. Input data was therefore more refined. However, the number of excavation stages was still limited, since no final designs were yet developed for the cavern.

The horizontal stress distribution, joint pattern and general input data used in Phase II studies with UDEC-BB are illustrated in Figure 10. Two models were run, the first with 25m of overburden, the second with 45m of overburden, to represent different vertical cross-sections. Only three excavation stages were modelled in each case.

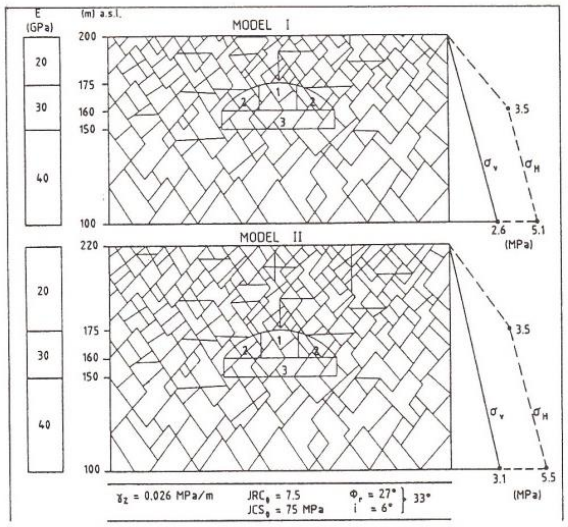

Fig. 10 Phase II assumptions concerning boundary stress conditions, deformation modulus (E) and joint properties. Model I = 25m overburden, Model II = 45m overburden.

The assumed level of horizontal stress used in Phase II modelling lies close to the major stress line presented in Figure 7. While this may appear a non-conservative assumption, it is supported by hydraulic fracturing stress measurements of 4.0 MPa and 2.6 MPa at elevation 150 m.a.s.l., and by overcoring measurements of 4.3 MPa and 3.4 MPa for major and intermediate stress at the same elevation (with uncertain excavation effect). A number of shut-in tests using joint jacking gave values of 3.0 MPa as high as elevation 180 m.a.s.l. Favourable horizontal stress levels are therefore apparent along both axes.

Graphical presentation of the UDEC-BB results will only be given for Model I which had the minimum overburden of 25 metres. However, results for Model II will also be given in simplified tabular form, so that comparisons between the two depths can be made.

a) Stress Distribution caused by Excavation

Figure 11 illustrates the redistribution of stresses caused by the three stages of excavation. Relatively stress-free blocks are evident in immediate proximity to the arch. In practice such blocks would be secured by the systematic rock bolting. Smaller scale versions of the same phenomenon would be secured by the shotcrete, generally fibre reinforced.

b) Deformation caused by Excavation

Figure 12 illustrates the deformation that occurs as a result of the three stages of excavation. Table 3 summarises the maximum deformations recorded (in mm) for the three excavation stages, both for Models I and II (25 and 45 overburden).

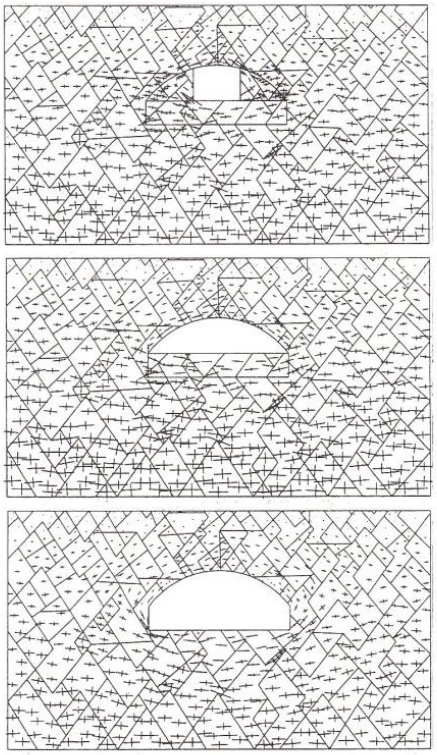

Fig. 11 Phase II UDEC-BB runs for Model I: Principal stresses.

Table 3. Summary of maximum deformations (mm)

Model No.	Overburden (m)	Cavern dimension (in m×m)		
		20×15	60×15	60×25
I	25	1.8	2.0	4.8
II	45	2.4	3.8	5.3

Results are similar to those obtained with simplified models in Phase 1, for the cases with k_0 = 1 and 3.

Maximum deformations of about 2mm in the first stages of excavation are caused by gravitational (and perhaps stress driven) instability of two wedge-shaped blocks in the arch. These stabilised after about 1.5 to 2.0mm shear, due to the dilation that occurs on the simulated non-planar joints. The BB-Lotus model of joint behaviour predicts peak friction mobilization after about 2mm of dilatant shear with the assumed block size, and this is clearly operative in the joint sub-routine in UDEC-BB.

The very small deformations calculated with both models suggests that the present depth, span, stress conditions and joint character are favourable for the very large span.

c) Shear Deformation Along Joints caused by Excavation

The relatively complicated behaviour of a jointed rock mass (even in two-dimensions) is quite well illustrated by the successive

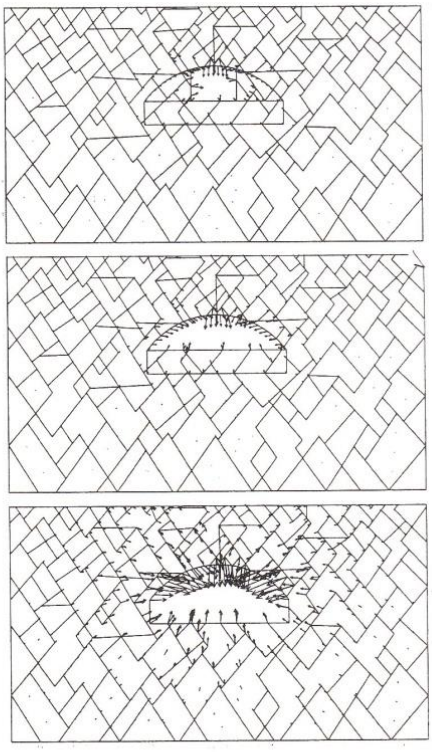

Fig. 12 Phase II UDEC-BB runs for Model I: deformation vectors (maximum 4.8mm).

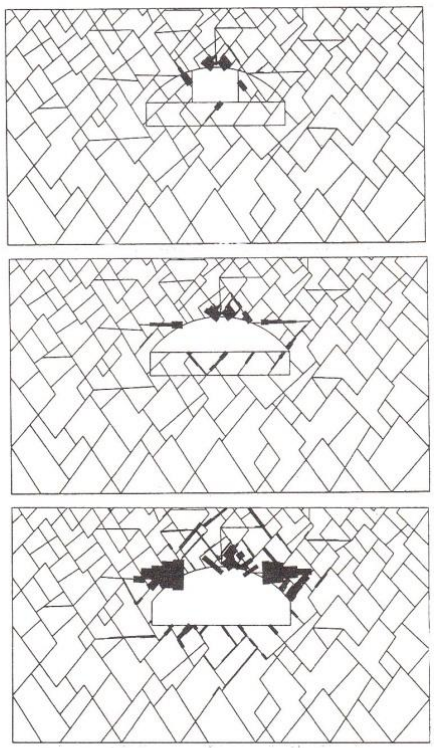

Fig. 13 Phase II UDEC-BB runs for Model I: joint shearing magnitudes (maximum 3.4mm).

developments of joint shearing seen in Figure 13. Maximum values for both Models I and II are listed in Table 4.

Table 4. Summary of maximum joint shear deformations (mm)

Model No.	Overburden (m)	Cavern dimension (in m×m)		
		20×15	60×15	60×25
I	25	1.5	1.9	3.4
II	45	2.0	2.8	3.2

Marked shear deformation is evident along the joints defining the wedge-shaped blocks referred to earlier. However, the maximum joint shearing magnitudes (3.2 to 3.4mm) are experienced along the horizontal joints at each side of the arch, once these are exposed by excavation. The third stage of excavation (benching downwards by 10m) causes almost a five-fold increase of these particular shear displacements, which would be resisted in practice by the systematic bolting of the arch and haunches. Slight shear deformations (small fractions of a mm) are registered right up to the surface, even in the model with 45m overburden. Again, these would tend to be minimized if systematic numerical bolting had been applied. (See Phase III modelling for results of bolting.)

d) Joint Conducting Apertures

Other graphical output from the UDEC-BB modelling indicates the locations of enhanced joint conductivity or rock mass permeability, and their magnitudes. Enhancement of permeability generally occurs in the axial direction, due to block displacement effects at quite a large number of joint intersections. Small, rectangular channels formed at these locations have maximum apertures ranging from 1.2 to 1.9mm, compared to the initial joint apertures of about 24 μm.

UDEC-BB MODELLING (PHASE III)

a) Introduction

During cavern construction, which started in April 1991, NGI's role was research coordinator of rock mechanics and engineering geology. The opportunity was provided to follow the actual stages of excavation, and also to model the influence of three new adjacent caverns, which have been excavated since January 1992, for the Norwegian Postal Services.

The UDEC -BB model geometry used in the third phase of modelling is shown in Figure 14. Phase III modelling was also predictive (Class A); the same basic joint geometry, input data and boundary stress conditions were applied to the Phase III model as those shown in Figure 10 (Phase II).

A diagram of the bolting pattern and excavation sequence that was modelled is shown in Figure 15.

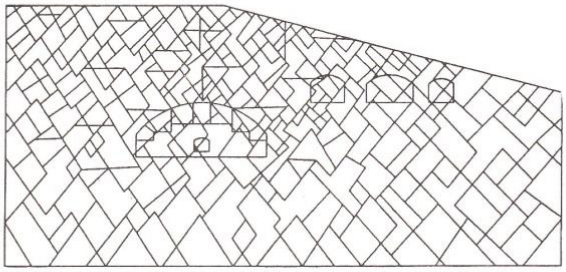

Fig. 14 Phase III UDEC-BB model, showing additional Postal Service caverns.

b) Bolt Reinforcement

The numbers in the cavern area refer to the excavation steps. The rock mass in the cavern arch and the walls were numerically reinforced by untensioned fully grouted rock bolts and anchors after each numerical excavation step.

The permanent bolting in the arch consisted in general of alternate 6m rebar bolts and 12m twin-strand cables in a 2.5×2.5m pattern. The former have a diameter of 25mm and capacity of 22 tons, while the latter have a diameter of 12.5mm and capacity (for each strand) of 16.7 tons at yield.

The 6m bolts were placed before the 12m cable bolts in both the 10m span pilot tunnel arch and in the primary 35m span top heading. Five centimetres of steel fibre reinforced shotcrete was sprayed first, followed by another five centimetres to make the final 10 cm thickness. The shotcreting was by the wet process, using 50 kg/m^3 of 25mm EE steel fibres, with a concrete quality of 35 MPa. The fibre reinforced shotcrete has not been modelled numerically.

(In actual practice, 194×12m long cable bolts were set in the arch, and 66×10m long cable bolts were set in the walls. In addition, a total of 1174 CombiCoat corrosion protected 6 and 5m long bolts were set in the arch and walls plus 845 × 3m and 4m long temporary bolts and 1068m^3 of fibre reinforced shotcrete.)

In the UDEC-BB model, each of the excavation steps was first run to equilibrium without any use of reinforcement. When 100% of deformation was achieved, the point where approximately 50% of deformation had occurred was then back-tracked. The bolts were then installed in an attempt to allow for the elastic deformation that will have already occurred before bolt installation.

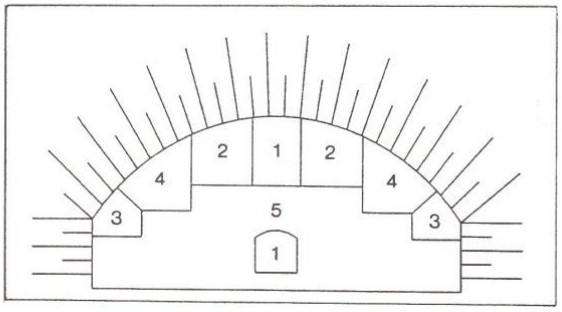

Fig. 15 Excavation sequence and bolting pattern.

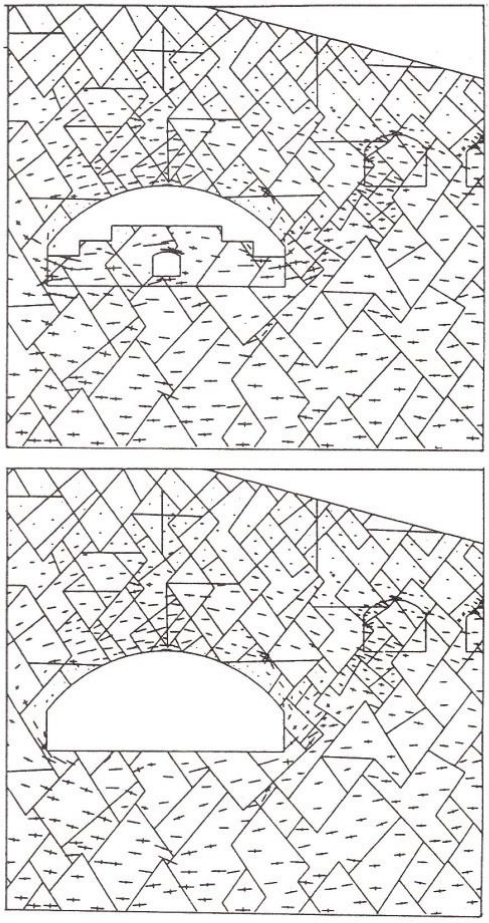

Fig. 16 Redistribution of principal stresses between the 4th and the 5th excavation steps, Phase III.

c) Stress Redistribution caused by Excavation

The UDEC-BB results for each of the excavated steps are given in Table 5. The redistribution of stresses that occurred between the 4th and 5th excavation step are shown in Figure 16.

In the arch of the cavern, some nearly stress free blocks can be observed. These blocks will be secured in practice by the systematic rock bolting. Shotcrete (fibre reinforced) which was not modelled in this study, will secure smaller blocks, representing the detailed joint structure.

d) Displacements caused by Excavation

Detailed results of displacement development at each stage of excavation are given in Table 5. In the central cavern arch, the maximum downward displacement at Stage 5 was 4.33mm. This increases slightly with each Postal Services cavern excavation, especially with the last. Figure 17 shows this development rather clearly. Presumably, the excavation of adjacent caverns gradually

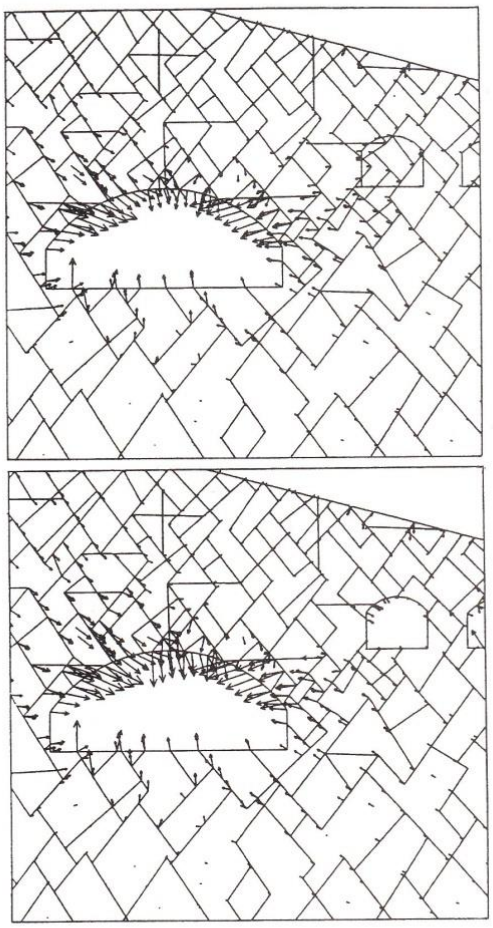

Fig. 17 Development of deformation vectors between the 5th excavation step and the excavation of the third Postal Service cavern.

Table 5. Summary of Gjøvik Ice Hockey Cavern run (with Postal Service caverns)

Parameter	Step 1	Step 2	Step 3	Step 4	Step 5	Excav. of 1st cavern	Excav. of 2nd cavern	Excav. of 3rd cavern
Max. Stress MPa	9.29	11.49	9.91	8.39	8.37	8.56	8.71	8.83
Displacements (mm)								
• maximum	1.85	1.80	2.63	6.99	8.16	8.28	8.43	8.65
• wall	-	-	-	1.33	3.78	3.88	3.92	3.97
• crown (vertical component)	0.50	1.08	2.62	4.05	4.33	4.39	4.87	7.01

reduces the horizontal stress levels and allows greater arch displacement. This effect was predicted by NGI prior to the decision to excavate the adjacent caverns, which fortunately were excavated at a higher level.

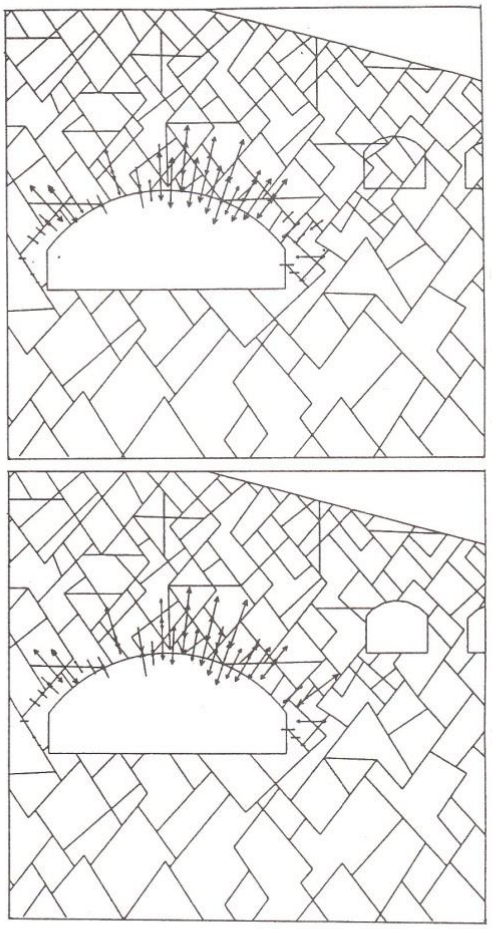

Fig. 18 Development of axial forces on the rock bolts between the 5th excavation step and the excavation of the third Postal Service cavern.

e) Bolt Load Development

Figure 18 illustrates the development of bolt loads for the 5 and 6m systematic bolting of the walls and arch, and for the 10 and 12m twin-strand cable bolts. Note that there are some increases of bolt loading for the 6m bolts caused by excavating the final Postal Services cavern. There are also one or two slight decreases in load.

DEFORMATION MONITORING AND COMPARISON WITH UDEC-BB RESULTS

NGI, NOTEBY, and SINTEF have all be involved in extensive monitoring studies. The near surface location of the cavern has meant that extensometers could be placed in boreholes from the surface using holes of 30 to 40m depth. Figure 19 shows the location of these extensometers (E1 to E7) which were installed prior to cavern construction, and reach to 1.5 or 2m above the cavern arch.

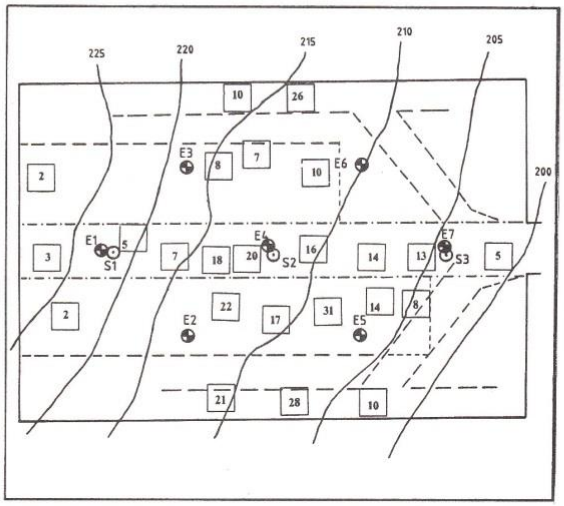

Fig. 19 Location of surface MPBX extensometers (E1 to E7) and cavern extensometers (S1 to S3) shown in relation to local rock mass Q-values (squares) as mapped in the cavern arch and access ramps.

Surface precision levelling was carried our at E1, E4 and E7 installations (above the cavern centre-line), and showed a gradual increase of subsidence to between 2.5 and 3mm during the four months it took to excavate the full 62m wide × 91m long × 8m high top heading. The initial deformations recorded by the six Interfels MPBX are shown in Figure 20. Some episodes of slight heave (arching upwards) are seen adjacent to excavation faces due to the high stresses. The centre of the cavern area (at E4) has subsided at this stage approximately 3mm relative to the surface 35m above. This 3mm has to be added to the surface subsidence of 2.5 to 3mm to obtain the preliminary net deformation.

A further source of deformation was the dilation of the blast damaged zone within the cavern. SINTEF's twin anchor S1 to S3 extensometer bolts of 2m and 13m length were located in the arch behind the advancing face in the 80m^2 pilot tunnel. They showed maximum values of 2.8, 1.3 and 2.9mm.

To obtain the maximum deformation of the centre of the arch, it is necessary to add E4 and S2 results to the maximum surface subsidence of approximately 4.5mm. A value of 8.2mm is obtained. The equivalent result at E1/S1 towards the SW end of the cavern is 7.0mm, and towards the NE end (E7/S3) the result is 7.5mm. (NOTEBY's sliding micrometer (E7) showed a total 2.23mm of deformation over its 28m length.)

Figure 21 shows the cumulative results for the three sets of instruments located along the cavern centre-line.

ROCK MASS QUALITY IN THE CAVERN

During core logging in pre-investigation studies, the mean Q-value calculated by means of data from boreholes gave a slightly higher rock quality than that found in the cavern. The difference in the two values is attributed to blasting which created artificial joints and opened up healed joints.

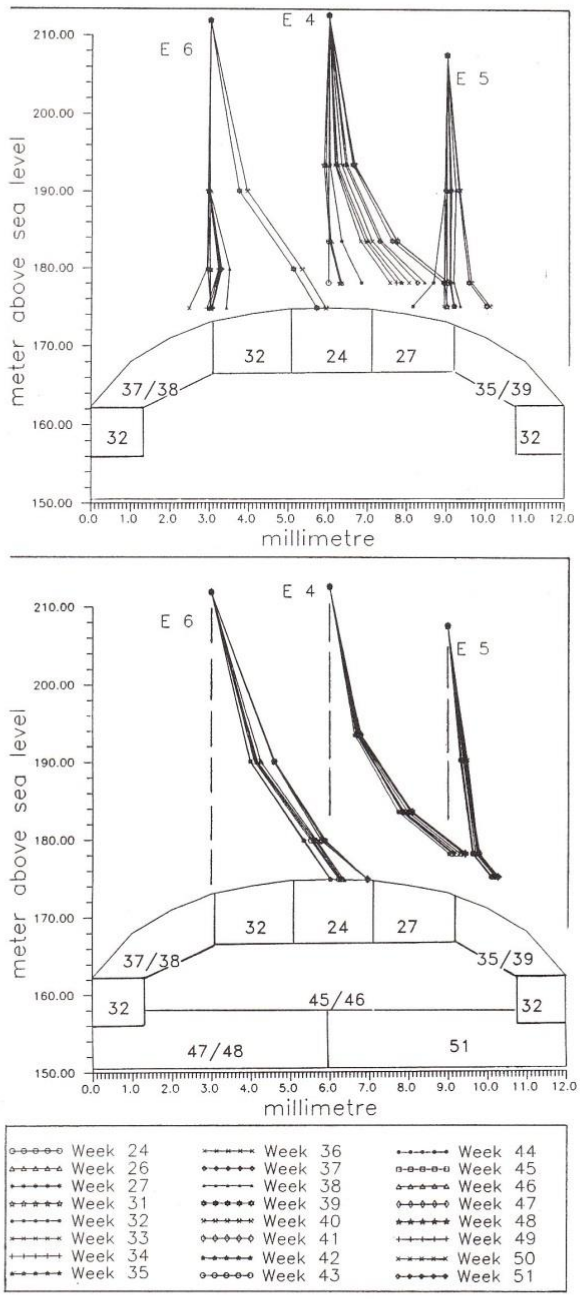

Fig. 20 Six MPBX installed from the surface prior to construction, monitored the weekly excavation. (Heave to the left, subsidence to the right). Results for E4, E5 and E6.

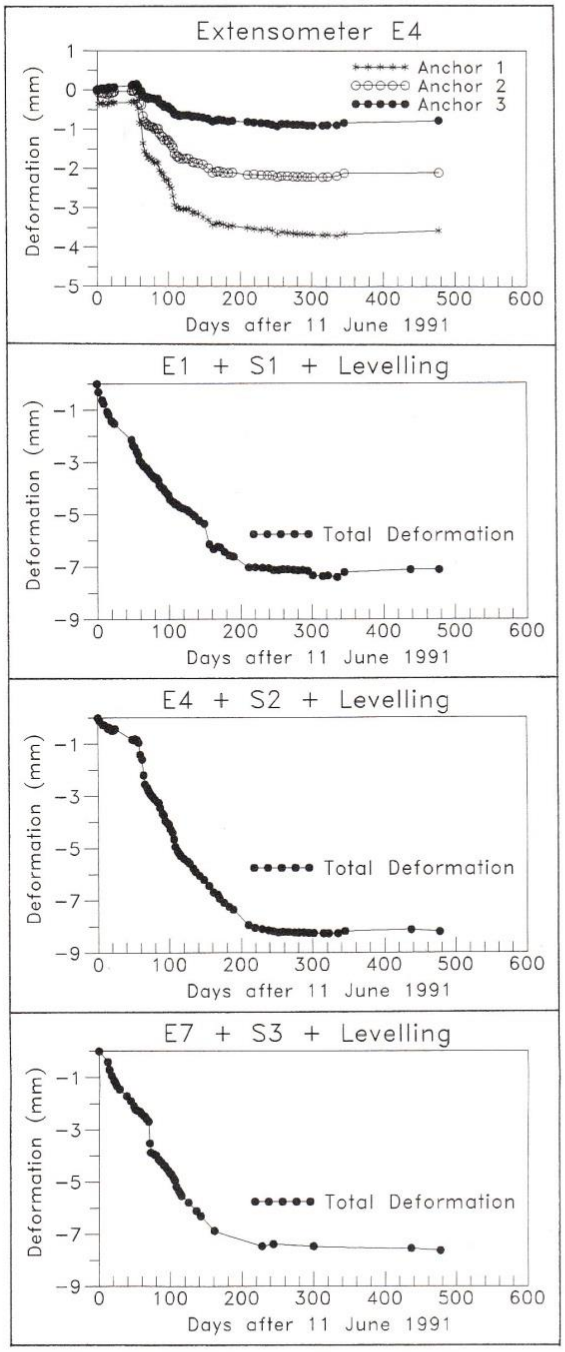

Fig. 21 Cumulative displacements along the cavern arch centre-line. The Olympic cavern was completely excavated at 200 days, the Postal Service caverns at 350 days. (7.0, 8.2 and 7.5mm = maximum centre-line displacements.)

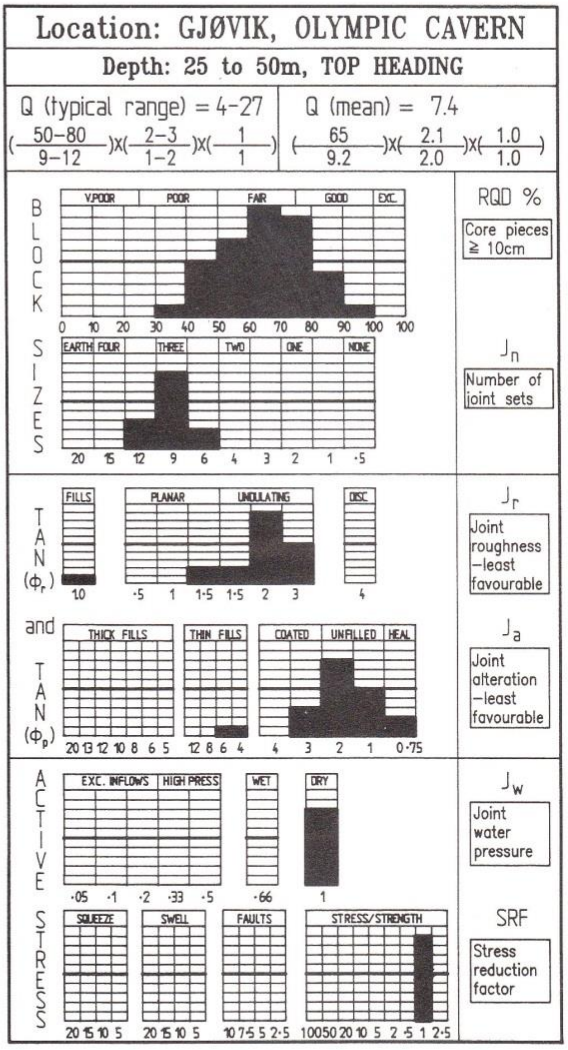

Fig. 22 Q-logging in the top heading (LØSET & BHASIN, 1991)

The rock in the cavern is red and grey jointed gneiss of PreCambrian age with 25 to 50m overburden. The average RQD (Rock Quality Designation) of 60-70% represents a fair rock quality. The PreCambrian gneiss has a network of micro-joints and isolated zones with clay fillings. The geotechnical investigations during the construction involved registration of rock quality using the Q-system and detailed joint surveys in the excavated portions of the cavern provided data on joint orientations, joint conditions and spacing. Measurements of strike and dip of the main discontinuities were made throughout the cavern. Data from 35 areas which together make up the majority of the upper part of the cavern were collected (LØSET AND BHASIN, 1991) and the relevant Q-values are shown in Figure 19 (see numbers in squares). These confirm the lower quality of rock at the ends of the cavern, as seen in the cross-hole seismic tomography (Figure 6).

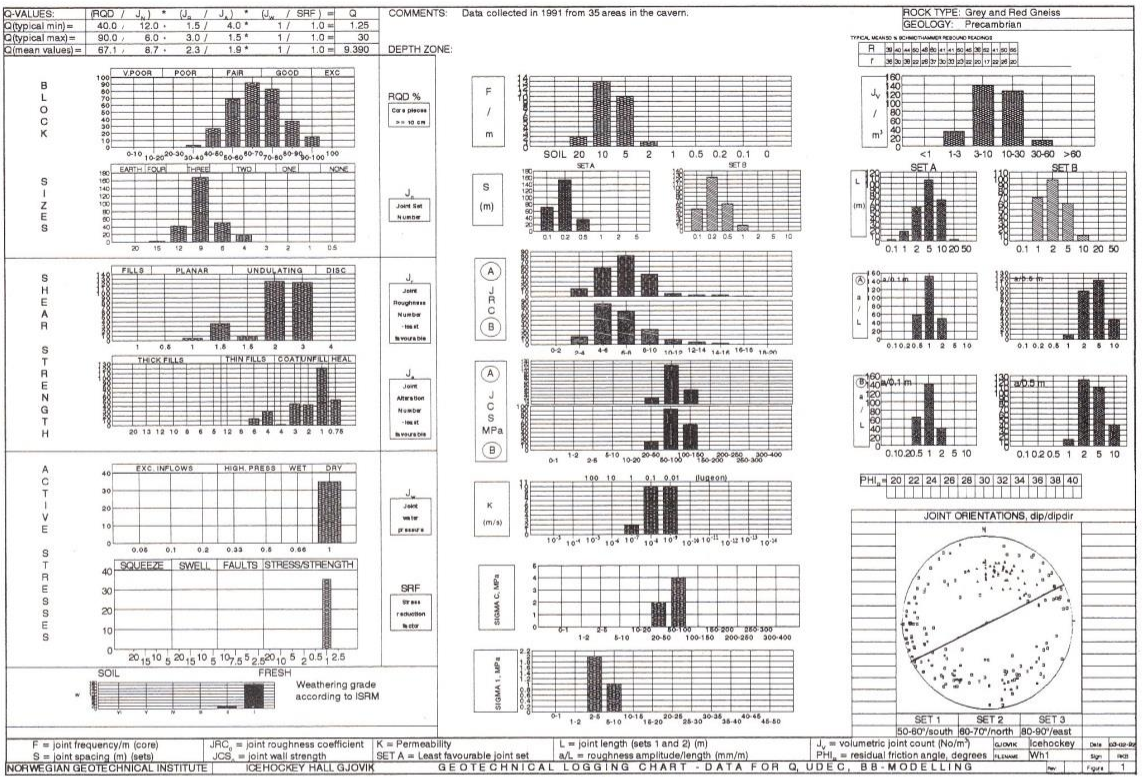

Fig. 23 Geotechnical logging results for the arch of the Olympic cavern. (LØSET & BHASIN, 1991)

a) Geotechnical Logging Charts

Key geological parameters including the Q-system data for rock mass classification and for subsequent jointed rock modelling studies have been recorded in histograms as shown in Figures 22 and 23. This method of recording the six Q-system parameters and other geotechnical information during field work for small or large areas has been found to be very useful. Incorporating all the information in a PC-based spread sheet makes it possible to see the variation in the different parameters through the cavern. Hence, data from different areas may be manipulated and combined. The geotechnical chart contains information for setting up input data files for numerical modelling of critical sections of the cavern.

The jointing in the cavern is irregular, rough walled and with quite large variations in dip and strike. These joint properties along with the rather high horizontal stresses of about 3.5 to 4 MPa at a depth of 45m below the surface (and perpendicular to the long axis of the hall) have been found to be very favourable for the stability of the cavern, and explain the rather moderate displacement magnitudes.

b) Displacements Compared with Q-Data Base

The range of Q-values obtained in the cavern and the corresponding range of displacements recorded by MPBX, provides information for comparing data with Q-system case records (BARTON et al. 1980). An updated plot of results for Q/SPAN (in metres) versus deformation is shown in Figure 24.

In general, the results are on the low side, and emphasise the positive effect of the high horizontal stress. In retrospect, the mean Q value for the top heading (7.4) and for the arch as a whole (9.4) could perhaps be adjusted by a more favourable estimate of SRF = 0.5 (favourable high stress). This value is seen to the left of the assumed value of 1.0 shown in Figure 23.

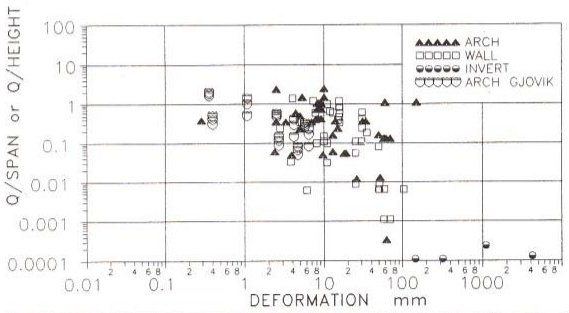

Fig. 24 Olympic cavern arch displacements compared to Q-system data base.

CONCLUSIONS

1. An exceptionally large span (62m) rock cavern has been constructed in rock of poor to fair to good quality ($Q \approx 1$ to 31). Mean Q values observed in phase I mapping prior to construction were 12 and the predicted range was 1 to 31. Mean Q values observed in the cavern pilot tunnel of $80m^2$ cross-section were 7.4 (typical range 4-27), and in the cavern arch as a whole 9.4. The typical range observed here was 1 to 30 as predicted.
2. Key properties favourable to large cavern construction have been the high horizontal stresses and the relative roughness or waviness of foliation planes and of the more continuous joints. The B and S(fr) method of rock reinforcement has taken care of less favourable features such as the less favourable joint orientations and mean RQD's of only 65 to 70% in the disturbed rock exposed by the blasting.
3. The usefulness of rock mass characterisation, cross-hole seismic tomography and rock stress measurements has been demonstrated by the good definition of input data for forward prediction (class A) modelling. Four different methods of deformation measurements have confirmed the relatively small deformations, that were predicted by UDEC-BB to be as little as 5mm (Phase II simplified model) and as large as 8mm (Phase III, realistic excavation sequence).
4. Precision levelling of the MPBX instrument heads at the surface, combined with deformation measurement throughout 30 to 40m of rock overlying the cavern indicate maximum deformations in the range 7 to 8mm along the cavern arch centre-line.
5. The combination of high stress and shallow location place the cavern close to the balance point between upwards and downward deformation as demonstrated by earlier physical models and FEM analyses.
6. The effective prediction of behaviour prior to cavern design, the efficient excavation and rock reinforcement, and the continuous monitoring of behaviour have provided confidence in the project and have been instrumental in its completion ahead of schedule and within budget.

ACKNOWLEDGEMENTS

The contributors to a paper describing this special project number many more than the nine authors listed. Significant contributions to the article have been received from colleagues at NOTEBY, SINTEF, and NGI. The authors would also like to thank members of the User Group who have provided generous support of the project: Veidekke and Selmer (whose JV were responsible for cavern construction), Dyno Industries, Fortifikasjon, NOTEBY, SINTEF, NGI, Østlandsforskning, the Municipality of Gjøvik, Statoil, Statkraft, Televerket, BeFo (Sweden).

REFERENCES

BARTON, N. and H. HANSTEEN (1979). *Very large span openings at shallow depth: Deformation magnitudes from jointed models and F.E. analysis*, Proc. 4th Rapid Excavation and Tunnelling Conference. Atlanta, Ch. 77, pp. 1331-1353.

BARTON, N., F. LØSET, R. LIEN AND J. LUNDE (1980). *Application of the Q-system in design decisions concerning dimensions and appropriate support for underground installations*, Int. Conf. on Sub-surface Space, Rockstore, Stockholm, Sub-surface Space, Vol.2, pp. 553-561.

BARTON, N. (1983). *Application of Q-System and Index Tests to Estimate Shear Strength and Deformability of Rock Masses.* Proc.- International Symp. on Engineering Geology and Underground Construction, Lisboa, Vol. 2, pp. II.51-II.70.

BARTON, N. AND S.C. BANDIS (1990). *Review of predictive capabilities of JRC-JCS model in engineering practice.* International Symposium on Rock Joints. Loen 1990. Proceedings, pp. 603-610.

BARTON, N. (1991). *Geotechnical Design.* WT Focus, World Tunnelling, November 1991.

BARTON, N., E. GRIMSTAD, G. AAS, O.A. OPSAHL, A. BAKKEN, L. PEDERSEN and E.D. JOHANSEN (1992). *Norwegian Method of Tunnelling.* WT Focus, World Tunnelling, June and August 1992.

BIENIAWSKI, Z.T. (1976). *Rock mass classification in rock engineering*, Proc. Symposium on Exploration for rock Engineering, Johannesburg, Volume 1, pages 97-106.

BROWN, E.T. and E. HOEK (1978). *Trends in relationships between measured in situ stresses and depth.* International Journal of Rock Mech. and Min. Sci & Geomech. Abstracts, Vol. 15, pp. 211-215.

BY, T.L. (1987). *Geotomography for rock mass characterisation and prediction of seepage problems for two main road tunnels under the City of Oslo.* Proc. Int. Cong. on Rock Mech. (ISRM). Montreal, Canada pp. 37-40.

CUNDALL, P.A. (1980). *A generalized distinct element program for modelling jointed rock.* Report PCAR-1-80, Contract DAJA37-79-C-0548, European Research Office, US Army. Peter Cundall Associates.

GRIMSTAD, E., N. BARTON, R. LIEN, J. LUNDE, and F. LØSET (1986). *Classification of Rock Masses with Respect to Tunnel Stability-New Experiences with the Q-system* (In Norwegian). Fjellsprengningsteknikk, Bergmekanikk, Geoteknikk, p. 30.1 - 3.18 Tapir Press, 1986.

LØSET, F. AND R. BHASIN (1991). *Engineering Geology - Gjøvik Ice Hockey Cavern.* Research Project: "Publikumshall i Berg". SINTEF/NGI/ØSTLANDSFORSKNING.

MAKURAT, A., N. BARTON, G. VIK., P. CHRYSSANTHAKIS AND K. MONSEN (1990). *Jointed rock mass modelling.* International Symposium on Rock Joints. Loen 1990. Proceedings, pp. 647-656.